

Quantitative Metallographic Parameters to Describe Microstructures of Multiphase Materials

André Luiz Moraes Alves^{a*} , Wesley Luiz da Silva Assis^b, Paulo Rangel Rios^b 

^aUniversidade Federal do Rio de Janeiro, Escola Politécnica, Centro de Tecnologia, Departamento de Engenharia Metalúrgica e de Materiais, Av. Horácio Macedo, 2030, Bloco F, Cidade Universitária, 21941-598, Rio de Janeiro, RJ, Brasil.

^bUniversidade Federal Fluminense, Escola de Engenharia Industrial Metalúrgica de Volta Redonda, Av. dos Trabalhadores, 420, 27255-125, Volta Redonda, RJ, Brasil.

Received: November 08, 2022; Accepted: January 29, 2023

One typically characterizes the transformation kinetics of a parent phase, α , into a single phase, β , by measuring the volume fraction transformed, V_V^β , against time. Sometimes one also reports the interfacial area density between the new and the parent phase, $S_V^{\alpha\beta}$, against the volume fraction transformed. $S_V^{\alpha\beta}$ is a dynamic interface. It migrates as the growth of the new phase takes place. Interfaces between transformed phases might be called static interfaces. These may be present before transformation starts, for example, grain boundaries of a polycrystalline parent phase. Alternatively, static interfaces, $S_V^{\beta\beta}$, may appear during the transformation because of impingement. Therefore, one may better understand the microstructural evolution following the behavior of the volume fraction, dynamic and static interfaces. A more complicated situation occurs if the parent phase transforms into two or more product phases, for example, $\alpha \rightarrow \beta, \gamma$. In this work, we apply parameters to describe the transformation of a parent phase into a single phase, the contiguity and the dispersion, to the situation in which the parent phase transforms into two or more phases. We tested these parameters against computer simulations and concluded that they combine a good description of the behavior of the simulated transformations and simplicity.

Keywords: phase transformations, recrystallization, simultaneous and sequential transformations, computer simulation, microstructures, quantitative parameters.

1. Introduction

One typically characterizes transformation kinetics by measuring the volume fraction transformed, V_V , as a function of time. The analysis of the kinetics is the basis for understanding the transformation. Still, one may gather substantial information about the transformation from its microstructural evolution over time. Therefore, a more thorough understanding of the transformation requires additional microstructural parameters. Considerable progress has been made in characterization techniques, notably 3-d techniques. Nonetheless, quantitative metallographic measurements on a planar section are still widely employed for their simplicity and low cost.

Specifically, the most common situation is transforming a polycrystalline parent phase, p , into several single-phase regions, denoted phase 1. In this case, in addition to V_V , quantities related to the interfaces between the phases may be easily obtained. Namely, the interfacial area density between a) parent phase and phase 1, S_V or S_V^{1p} ; b) In a polycrystal, parent phase and parent phase, S_V^{pp} ; c) phase 1 and phase 1, S_V^{11} .

By far the most commonly reported measurement, after V_V , is that of S_V . A plot of S_V against V_V is the so-called *microstructural path*^{1,2}. S_V or S_V^{1p} is the interface between phase 1 and the parent phase. It is a *dynamic* interface. It migrates

as phase 1 growth takes place. There is also another kind of interface: the *static* interface. They may be present before the transformation starts, as is the case of the grain boundaries, S_V^{pp} , of a polycrystalline parent phase. Alternatively, they may appear during transformation because of the impingement. For example, growing regions of phases 1 and 1 may impinge on each other. From this impingement, a static interface between phase 1 and phase 1, S_V^{11} , appears. The behavior of these static interfaces during the transformation may provide valuable information on the microstructural evolution. The behavior of S_V^{11} shows how the impingement is taking place. The impingement is related to the location of the nuclei of phase 1 within the parent phase.

One may define several parameters by considering these static interfaces³.

In a previous work⁴, with the help of computer simulation, we examined a situation in which a single phase formed on the grain boundaries of a parent phase. That work⁴ concluded that in addition to V_V and S_V two other parameters were good choices for a more thorough description of the microstructural evolution. One is the so-called contiguity of phase 1

$$C_1 = \frac{2S_V^{11}}{2S_V^{11} + S_V^{1p}} \quad (1)$$

* e-mail: andrealves@metalmat.ufjf.br

The contiguity essentially captures the behavior of the interfaces between the same phase. The contiguity has interesting properties, especially regarding the onset of impingement, see⁴⁻⁷. Equation 1, the contiguity, varies from zero to one as the volume fraction transformed varies from zero to one.

The second is the dispersion parameter, δ , defined by Hornbogen³:

$$\delta = \frac{S_V^{1P}}{S_V^{PP}} \quad (2)$$

The dispersion parameter measures the ratio of interfaces between distinct phases to interfaces between the parent phase. The inconvenience of the above definition is that the dispersion tends to infinity as the volume fraction transformed tends to one. Equation 2 behaves in this way because S_V^{PP} tends to zero⁴.

A more complicated situation is when two or more phases form from a parent phase. The formation of those two new phases may take place by simultaneous or sequential transformations^{8,9}. For example, consider the situation in which three phases are present: parent, phase 1, and phase 2. The main difference from the case where only one phase forms from a parent phase is that one now has significantly more interfaces. Indeed, in addition to the volume fractions of phases 1 and 2, there are six interfacial area densities instead of two. Those interfacial area densities are: S_V^{11} , between phase 1 and phase 1; S_V^{22} , between phase 2 and phase 2; S_V^{12} , between phase 1 and phase 2; S_V^{1P} , between phase 1 and the parent phase; S_V^{2P} between phase 2 and the parent phase and S_V^{PP} , the grain boundary area of the parent phase.

This article aims to generalize our previously published paper⁴. Here we suggest the application of the parameters defined above for the situation in which two or more phases form from a parent phase. We test these parameters applying to the situation in which a parent phase forms two phases. Three computer simulations of simple simultaneous and sequential transformations generated distinct microstructures used to perform the test.

2. Microstructural Descriptors for Multiphase Transformations

The first two parameters proposed are the contiguity of the same phase, C_{ii} , and the contiguity between different phases, C_{ij} . Our definitions here essentially retain the form of Equation 1. Thus, a natural extension of Equation 1 would be to keep its form and apply it to the other interfaces:

$$C_{ii} = \frac{2S_V^{ii}}{2S_V^{ii} + S_V^{iP}} \quad (3)$$

$$C_{ij} = \frac{2S_V^{ij}}{2S_V^{ij} + S_V^{iP} + S_V^{jP}} \quad (4)$$

Where “ i ” and “ $j \neq i$ ” correspond to a product phase numbered from 1 to N .

In the same way, the following parameter proposed is the dispersion of each phase, δ_i . As one can see, this parameter

is formally identical to the dispersion parameter proposed by Hornbogen³, Equation 2.

$$\delta_i = \frac{S_V^{iP}}{S_V^{PP}} \quad (5)$$

The parameters defined by Equations 3-5a are applied to distinguish between:

- two simultaneous transformations in which each phase has the same number of nuclei and the same velocity. This simulation will be our “baseline,” as all parameters should be equal in this case;
- two simultaneous transformations in which phase 2 has ten times more nuclei than phase 1. In this case, we keep the $V_V^1 = V_V^2$ compensating the growth velocity of the phases;
- two sequential transformations with the same considerations of the case “a”; the only difference was that phase 2 started when phase 1 reached $V_V^1 = 0.1$.

It is worthy of note that the question is not only to measure and define parameters to characterize a transformation but parameters that are sensitive enough that their differences are above the experimental errors.

It is interesting to remark that some transformations might not be very sensitive to the kinetics curve, V_V vs. t or to the microstructural path, S_V vs. V_V curve. Our previous work⁴ shows this. Therefore, it is essential to be more precise about what the “sensitivity” of a parameter means in this context. If we were dealing with a purely mathematical issue, two numbers are either equal or not. If two numbers differ by any amount, say, by 0.1% or 0.001%, they are not equal. However, when one is talking about experimentally determined quantities, the situation is different. That is so because experimental quantities exhibit *experimental errors*. For example, $\pm 5\%$ is a reasonable experimental error for good metallographic practice. Therefore, if a parameter differs from another by 2% for two transformations, it is not very useful to distinguish between them as this difference is well below the experimental errors. Therefore, the question is not only to measure and define parameters to characterize a transformation but parameters that are sensitive enough that their differences are above the experimental errors. In this regard, determining parameters from computer simulations can be helpful. This is because computer simulations are free from experimental errors.

3. Computer Simulation Methodology

Nucleation and growth transformations were computer-simulated in 3-d using the causal cone method^{10,11}. The simulations employed a cubic matrix comprising $300 \mu\text{m} \times 300 \mu\text{m} \times 300 \mu\text{m}$ with periodic boundary conditions. Each cubic cell edge length was equal to $1 \mu\text{m}$. 128 nuclei distributed in space by a homogeneous Poisson point process^{12,13} generated the polycrystalline parent phase. Therefore, the parent phase had 128 grains with a mean grain size of $60 \mu\text{m}$. We did three simulations corresponding to cases a to c of the previous

section. It is essential to mention that for all simulations presented in this work, one carried out 50 simulation runs. The plots shown below were the mean value of the data of those 50 simulations. We used 50 simulations as our previous computer simulation experience has shown this to be a sufficiently high number of runs for reliable statistical means. The following section includes more details about the simulations themselves.

4. Simulated Microstructures for the Cases in Which the Parent Phase Transforms into Two Phases

Figures 1a and 1b show the simulated microstructure of the parent phase, “*p*,” before transforming into the two product phases. The transformation of the parent phase into two product phases may take place simultaneously or sequentially^{8,9}. In the simulations carried out here, the nucleation was always site-saturated. Furthermore, the nuclei were distributed according to a homogeneous Poisson point process^{12,13}.

Two simulations of simultaneous transformations and one of the sequential transformations were carried out. Thus, the parent phase “*p*” depicted in Figures 1a and 1b transformed into phases “1” and “2”. Therefore, at the beginning of the transformation, one had a single phase: the parent phase; during the transformation, one had three phases: *p*, 1, and 2; and finally, as the matrix transformation ended, only phases 1 and 2 remained.

The simulation of the first simultaneous transformation was carried out for reference purposes. The product phases, phases 1 and 2, had the same number of initial nuclei, N_1 and N_2 , equal to 64. These values were chosen to obtain a grain size of phases 1 and 2 (mean intercept length) in the fully transformed matrix approximately equal to 60 μm . The phases also have the same growth velocities, G_1 and G_2 ,

equal to 1 $\mu\text{m}/\text{unit of time}$. Notice that each phase, 1 and 2, obeys the JMAK equation for site-saturated nucleation in the simultaneous transformations. Phase 1 kinetics, V_V^1 vs. time, t , is given by:

$$V_V^1 = 1 - \exp\left(-\frac{4\pi}{3} N_1 G_1^3 t^3\right) \quad (6)$$

with a similar expression for V_V^2 . Evidently, in this case, the kinetics was the same for both phases, resulting in $V_V^1 = V_V^2$. The simulation of the sequential transformation used the same parameters. The significant difference between the simultaneous and sequential transformation was that in the sequential transformation, phase 2 started to form only when phase 1 reached $V_V^1 = \bar{v}$. The second simultaneous transformation simulation used parameters chosen in such a way that phases 1 and 2 would have the same kinetics with $V_V^1 = V_V^2$ but a different microstructure. Thus, in the simulation of the simultaneous transformation described in “b” above, the initial number of nuclei was $N_1 = 64$ and $N_2 = 640$, with

$$G_1 = 1 \mu\text{m}/\text{unit of time and } G_2 = \sqrt[3]{\frac{N_1 G_1^3}{N_2}} \cong 0.46 \mu\text{m}/\text{unit of}$$

time. This choice of parameters meant that $N_1 G_1^3 = N_2 G_2^3$ and therefore $V_V^1 = V_V^2$ (see Equation 6). The smaller velocity and higher number of nuclei of phase 2 meant that phase 2 had a higher number of smaller transformed regions than phase 1. Consequently, this resulted in phase 1 and phase 2 having identical kinetics but distinct microstructures. By contrast, in the first simulation of simultaneous transformations, the kinetics and the microstructures were identical. The simulation of the simultaneous transformations was that the parameters could be compared, keeping the kinetics the same for both phases.

Figures 2a-c show the simulated microstructures for simultaneous and sequential transformations. Again, the difference between the microstructures of the three simulated cases is noticeable.

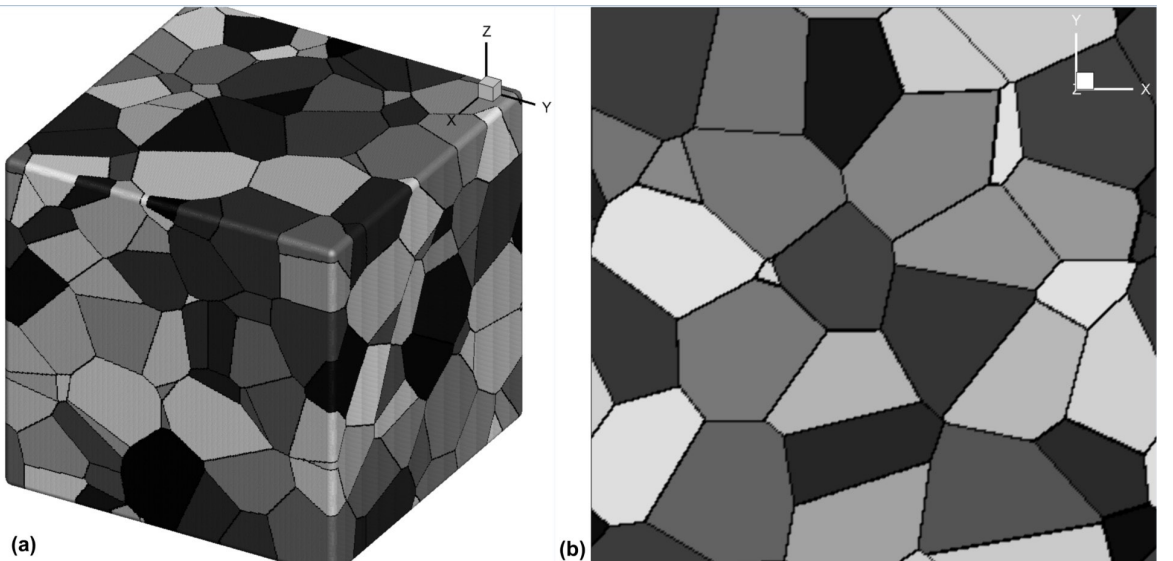


Figure 1. Representation of simulated microstructure of the polycrystalline parent phase before transforming into the product phases. (a) 3-d simulated microstructure. (b) 2-d cross-section when the matrix is fully transformed where the grain boundaries correspond to S^{pp} .

5. Application of the Microstructural Descriptors for the Cases in Which the Parent Phase Transforms into Two Phases

We limit our discussion to the parameters presented in the introduction. However, of course, many other parameters may be defined. Therefore, we provide a list of possible parameters in the Appendix. We plotted the curves for *all* those listed parameters for the simulated cases. The conclusion was that the parameters defined by Equations 3-5 were better suited for their simplicity and ability to distinguish the microstructures. Thus, in what follows, we focus on the parameters defined by Equations 3-5.

Figures 3a-c show the kinetics of simultaneous and sequential transformations. For a more detailed study of sequential transformations, the reader is referred to Alves et al.⁸ As was mentioned above, in both simultaneous transformations, one had $V_V^1 = V_V^2$, so the kinetics curves were very similar. Figure 3a and 3b show that phases 1 and 2 have the same kinetics, as expected. In contrast, in Figure 3c, even if phase 2 starts to transform after phase 1 reaches only $V_V^1 = 0.1$, the kinetics of phase 1 and 2 were significantly different.

Figures 4a-c show the *microstructural path* of the simultaneous and sequential transformations. As expected, the microstructural path of phases 1 and 2 from the first simulation of simultaneous transformations are identical. Figure 4b is more critical as it shows the difference between

the microstructural path of phases 1 and 2 for the second simultaneous transformation. Both phases 1 and 2 always have the same volume fraction. However, phase 2 has more nuclei, so its volume fraction is composed of a higher number of smaller regions than the volume fraction of phase 1. Therefore, the interfacial area of phase 2 is always above that of phase 1, as shown in Figure 4b. Phase 2 has a higher interfacial area density than phase 1. Hence, the total interfacial area for both phases is higher in Figure 4b than in Figure 4a. Apart from that, all curves in Figure 4b are typical site-saturated transformations. The curves are symmetrical, with a maximum very close to the midpoint of the transformation. In Figure 4c, the behavior is different. Phase 1 started earlier and has a much larger volume fraction and a much larger surface area (recall that in this simulation, the number of nuclei is the same for both phases). Even though the deviation is slight, the curves are not exactly symmetrical. The total interface area curve in Figure 4c tilts towards larger volume fractions. The effect is small, probably undetectable experimentally under the same conditions. However, it shows that the total volume fraction of the sequential transformation behaves differently from the exact site-saturation model, even if phases 1 and 2 nucleation are site-saturated.

Figures 5a-c show the behavior of the contiguity as a function of volume fraction for the three simulations carried out here. Note that there are two product phases; therefore, Equation 3 takes the form of C_{11} and C_{22} and Equation 4 takes

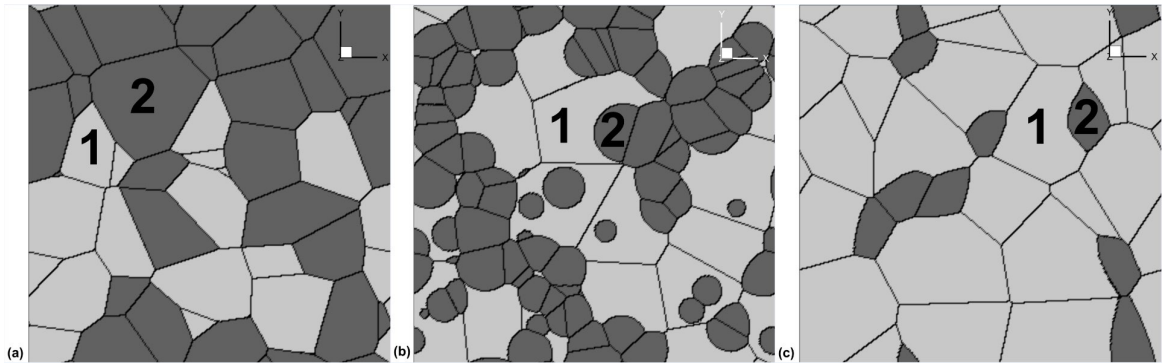


Figure 2. Representation of simulated microstructures showing a 2-d cross-section when the 3-d matrix is fully transformed. (a) simultaneous transformation with $N_1 = N_2 = 64$ and $G_1 = G_2 = 1 \mu\text{m}/\text{unit of time}$. (b) simultaneous transformation with $N_1 = 64$ and $N_2 = 640$ and $G_1 = 1 \mu\text{m}/\text{unit of time}$ and $G_2 \cong 0.46 \mu\text{m}/\text{unit of time}$. (c) sequential transformation, the only difference from the case shown in (a) is that phase 2 starts when phase 1 reaches $V_V^1 = 0.1$.

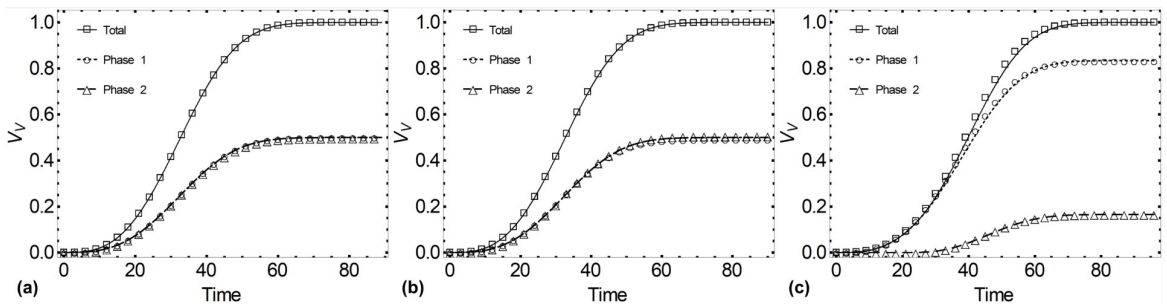


Figure 3. V_V versus time. (a) simultaneous transformation with $N_1 = N_2 = 64$ and $G_1 = G_2 = 1 \mu\text{m}/\text{unit of time}$. (b) simultaneous transformation with $N_1 = 64$ and $N_2 = 640$ and $G_1 = 1 \mu\text{m}/\text{unit of time}$ and $G_2 \cong 0.46 \mu\text{m}/\text{unit of time}$. (c) sequential transformation, the only difference from the case shown in (a) is that phase 2 starts when phase 1 reaches $V_V^1 = 0.1$.

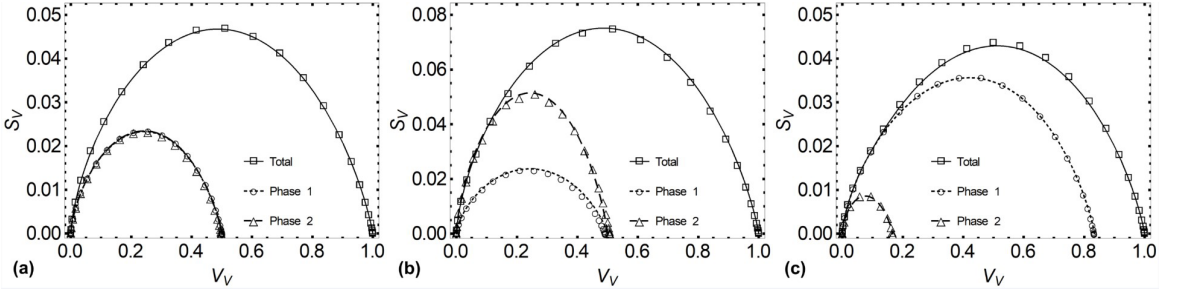


Figure 4. Microstructural Path. (a) simultaneous transformation with $N_1 = N_2 = 64$ and $G_1 = G_2 = 1 \mu\text{m/unit of time}$. (b) simultaneous transformation with $N_1 = 64$ and $N_2 = 640$ and $G_1 = 1 \mu\text{m/unit of time}$ and $G_2 \approx 0.46 \mu\text{m/unit of time}$. (c) sequential transformation, the only difference from the case shown in (a) is that phase 2 starts when phase 1 reaches $V_V^1 = 0.1$.

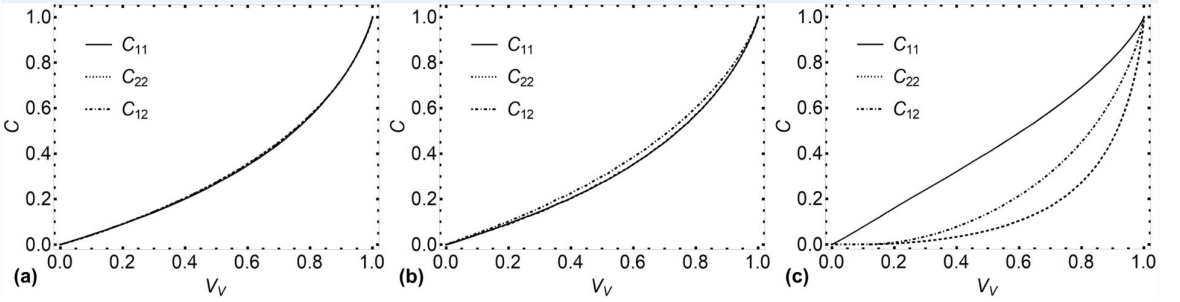


Figure 5. Contiguity of each phase versus V_V . (a) simultaneous transformation with $N_1 = N_2 = 64$ and $G_1 = G_2 = 1 \mu\text{m/unit of time}$. (b) simultaneous transformation with $N_1 = 64$ and $N_2 = 640$ and $G_1 = 1 \mu\text{m/unit of time}$ and $G_2 \approx 0.46 \mu\text{m/unit of time}$. (c) sequential transformation, the only difference from the case shown in (a) is that phase 2 starts when phase 1 reaches $V_V^1 = 0.1$.

the form of C_{12} . Figure 5a shows the result of the first simulation. Of course, as in this case, the number of nuclei is the same, and the velocity is the same, one would expect the contiguities C_{11} and C_{22} to be equal, as shown in Figure 5a. Nonetheless, Figure 5a depicts important information: C_{12} is the same as C_{11} and C_{22} . The contiguity resulting from the impingement between phases 1 and 2 has the same value as the contiguity resulting from the impingement between the same phase. Figure 5b shows that this behavior is similar to the second simultaneous transformation. The only discrepancy is that C_{12} is slightly higher than C_{11} and C_{22} . Figure 5b also shows that the contiguity C_{22} is also equal to C_{11} even though phase 2 has a higher area per unit of volume than phase 1. The contiguity relates to the arrangement of a phase in space. The contiguity should be the same if all regions are uniform randomly dispersed within the parent phase. However, if there is clustering, one observes a significant difference in contiguity⁵. In Figure 5c, the situation changes: C_{12} is higher than C_{22} but smaller than C_{11} . One possible reason for this is that in contrast with the simultaneous transformations the behavior of the volume fraction of the individual phases during the sequential transformation is very different. The volume fraction contribution of phase 1 to the total volume fraction is much higher than the corresponding volume fraction contribution of phase 2. This is a consequence of phase 2 starting to form later, see Figure 3b. Also, even though the nuclei are uniform randomly located in space, the fact that phase 1 starts earlier influences the spatial arrangement of phase 2 and, thus, its contiguity. We see C_{12} significantly higher than C_{22} because when phase 2 forms,

phase 1 is already there. Therefore, impingement between 1 and 2 starts earlier than between phase 2 and phase 2, leading to a higher C_{12} .

Figure 5 shows that the behavior of the multiphase contiguity is consistent with our definition and expected properties of the contiguity of two phases. Therefore, it shows that the generalization proposed here works well. For the present purposes, the main point is the ability of the contiguities to distinguish the behavior of the three kinds of interfaces.

Figures 6a-c show the dispersion parameter as a function of the total volume fraction. For these cases, Equation 5 takes the form of δ_1 and δ_2 . Figure 6a needs no comment as the number of nuclei and velocity of phases 1 and 2 are the same. Consequently, the value of the dispersion parameter must be the same for both phases. The situation changes in Figure 6b. In Figure 6b, the dispersion parameter of phase 2 reflects that phase 2 has more interfaces than phase 1. Therefore, the dispersion parameter of phase 2 is higher than the dispersion parameter of phase 1. In contrast with Figures 6a and 6b, Figure 6c shows that the dispersion of phase 1 is higher than the dispersion of phase 2. This is because the volume fraction of phase 1 is much higher than phase 2. A much higher volume fraction of phase 1 than of phase 2 means that the interfacial area density between phase 1 and the parent phase is much higher than the interfacial area density between phase 2 and the parent phase.

Notice that the dispersion parameter, Equation 5, also includes the grain boundary of the parent phase in the denominator so that it is sensitive to how or the rate the new

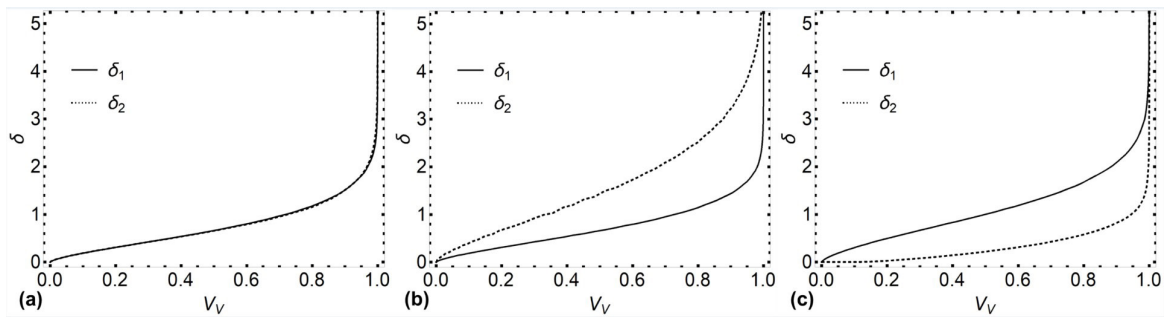


Figure 6. Dispersion of each phase versus V_V . (a) simultaneous transformation with $N_1 = N_2 = 64$ and $G_1 = G_2 = 1 \mu\text{m/unit of time}$. (b) simultaneous transformation with $N_1 = 64$ and $N_2 = 640$ and $G_1 = 1 \mu\text{m/unit of time}$ and $G_2 \cong 0.46 \mu\text{m/unit of time}$. (c) sequential transformation, the only difference from the case shown in (a) is that phase 2 starts when phase 1 reaches $V_V = 0.1$.

phases consume the grain boundaries. It is worthy of note that if one phase were nucleated on the grain boundaries, the grain boundaries of the parent phase would disappear much faster, with a substantial effect on the dispersion parameter.

It is worth mentioning that since there is a more significant number of interfacial area densities, it is possible to define the contiguity, the dispersion, and additional parameters in other ways. Other definitions of these parameters were used in previous work⁸. The problem of using definitions too far from the definitions presented in Equations 1-2 is how to interpret them. By using the definitions presented by Equations 3-5, based on Equations 1-2, the behavior of a microstructure containing two phases can be taken as the starting point for interpreting the microstructures containing three or more phases.

6. Conclusions

This work proposed several quantitative metallographic parameters to describe the microstructure and its behavior. Besides, there were other parameters that also apparently gave reasonable results, see Appendix. However, the ones defined in the body of the text were able to characterize and distinguish the multiphase transformations, combining reliable results, simplicity, and straightforward interpretation. In addition, our results permit the following conclusions:

- Two new parameters, contiguity, and dispersion, were defined here specifically for the situation in which a parent phase decomposes into two phases. For example, this decomposition could occur with phases 1 and 2 forming simultaneously or sequentially.
- We tested these parameters using microstructures generated by three computer simulations of simple cases. In all cases, the parameters behaved well and were quite distinct for each phase.
- We believe that the parameters defined here satisfactorily extend the parameters defined for a single phase forming from a parent phase and employed in previous work⁴.

7. Acknowledgments

This study was financed in part by the Coordenação de Aperfeiçoamento de Pessoal de Nível Superior - Brasil

(CAPES) - Finance Code 001. The authors are also grateful to Conselho Nacional de Desenvolvimento Científico e Tecnológico, CNPQ, and Fundação Carlos Chagas Filho de Amparo à Pesquisa do Estado do Rio de Janeiro, FAPERJ, for the financial support.

8. References

1. DeHoff RT. Annealing processes - recovery, recrystallization and grain growth. In: Hansen N, Juul Jensen D, Leffers T, Ralph B, editors. Risø national laboratory. Roskilde, Denmark; 1986. p. 35-52.
2. Gokhale AM, Iswaran CV, DeHoff RT. Use of the stereological counting measurements in testing theories of growth rates. *Metall Trans, A, Phys Metall Mater Sci.* 1979;10(9):1239-45.
3. Hornbogen E. On the microstructure of alloys. *Acta Metall.* 1984;32(5):615-27.
4. Da Fonseca GD, Da Silva Siqueira F, Alves ALM, Da Silva Assis WL, Rios PR. Microstructural descriptors to characterize computer simulated microstructures generated by nucleation on a Kelvin polyhedra network. *J Mater Res Technol.* 2018;7(3):337-41.
5. Vandermeer RA. Microstructural descriptors and the effects of nuclei clustering on recrystallization path kinetics. *Acta Mater.* 2005;53(5):1449-57.
6. Ventura HS, Alves ALM, Assis WLS, Villa E, Rios PR. Influence of an exclusion radius around each nucleus on the microstructure and transformation kinetics. *Materialia (Oxf).* 2018;2:167-75.
7. Rios PR, Pereira LO, Oliveira FF, Assis WLS, Castro JA. Impingement function for nucleation on non-random sites. *Acta Mater.* 2007;55(13):4339-48.
8. Alves ALM, Assis WLS, Rios PR. Computer simulation of sequential transformations. *Acta Mater.* 2017;126:451-68.
9. Rios PR, Villa E. Simultaneous and sequential transformations. *Acta Mater.* 2011;59(4):1632-43.
10. Cahn JW. The time cone method for nucleation and growth kinetics on a finite domain. *Proc MRS.* 1996;398:425-37.
11. Rios PR, Villa E. Application of stochastic geometry to nucleation and growth transformations. In: Molodov DA, editor. *Microstructural design of advanced engineering materials.* 1st ed. Weinheim-Germany: Wiley-VCH; 2013. p. 119-59.
12. Rios PR, Villa E. Transformation kinetics for inhomogeneous nucleation. *Acta Mater.* 2009;57(4):1199-208.
13. Chiu SN, Stoyan D, Kendall WS, Mecke J. *Stochastic geometry and its applications.* 3rd ed. Chichester, United Kingdom: Wiley; 2013.

Supplementary material

The following online material is available for this article:
Appendix